Sensorless Control of a Seven-phase Non-sinusoidal Permanent Magnet Synchronous Machine Using High Frequency Signal Injection Method

Y. Huang, J. Gong, Y. Zhu, F. Tan, W. Tian, E. Semail, N-K. Nguyen

Sensorless Control of a Seven-phase Non-sinusoidal Permanent Magnet Synchronous Machine Using High Frequency Signal Injection Method

Y. Huang, J. Gong, Y. Zhu, F. Tan, W. Tian
School of Electrical Engineering
Shandong University
Jinan, China
gongjinlin@sdu.edu.cn

E. Semail, N-k. Nguyen
Arts et Métiers ParisTech, *Centrale Lille, HEI*
Univ. Lille
Lille, France
eric.semail@ensam.eu

***Abstract*—this paper presents a sensorless control strategy for seven-phase non-sinusoidal permanent magnet synchronous machine (NSPMSM) with high frequency signal injection (HFSI) method in 5th harmonic subspace. Seven-phase non-sinusoidal machine benefits high torque density due to the use of third harmonic components. Firstly, two torque generation strategy in different harmonic subspaces with the minimum injected rms value and amplitude of current is deduced in this paper. Secondly, in order to reinforce the reliabilities of multiphase machine, the HFSI sensorless control is employed. Comparing with traditional HFSI method, the proposed control strategy is achieved in 5th harmonic subspace, which can avoid the torque ripple caused by the injected signal. Finally, according to simulations results the two torque distribution method is validated and compared and the effectiveness of the HFSI method is verified.**

Keywords—sensorless control; non-sinusoidal; multiphase; high frequency signal;

I. INTRODUCTION

In the field of aerospace and transportation, the reliability of motor drive system is one of the most concerned performance. Fault-tolerant control and sensorless control is the known ways to improve the reliability. With the development of power electronic, the motor drive system is not limited by 3-phase. Multiphase machine is used more widely in daily life, which has stronger fault-tolerant operation ability than three phase one[1,2].

In high performance drive system , a position sensor is usually necessary. Nevertheless, the use of sensor will increase the cost, the size of motor, the moment of inertia and reduce the operation reliability simultaneously. In order to enhance the reliability of drive system, sensorless control should be employed[3]. The HFSI method is usually applied to low-speed machine operation. However, with the injection of signal, the extra torque ripple will be produced[4].

In this paper, based on the advantages of the non-sinusoidal machine[5], two torque distribution methods in different harmonic subspace with minimum rms current and minimum amplitude current are deduced. And a sensorless control strategy with HFSI is proposed for a seven-phase NSPMSM in 5th harmonic subspace in order to avoid the extra torque ripples. The paper is organized as follows: In section II, the high frequency mathematic model of NSPMSM is given. In section III, two torque distribution methods are deduced with a given torque. Then the HFSI method is introduced in section IV and the simulation is shown in section V.

II. SEVEN-PHASE MOTOR MODEL

A. D-q Coordination Model of Motor

Considering the high order of harmonic components of the seven-phase PMSM, the voltage equation in *d-q* coordinate is expressed in(1).

Where $[u_0, u_{d1}, u_{q1}, u_{d3}, u_{q3}, u_{d5}, u_{q5}]$ are the voltages in different subspaces, $[i_0, i_{d1}, i_{q1}, i_{d3}, i_{q3}, i_{d5}, i_{q5}]$ are the currents components, $[L_0, L_{d1}, L_{q1}, L_{d3}, L_{q3}, L_{d5}, L_{q5}]$ are the inductances, $[\Psi_{md1}, \Psi_{mq1}, \Psi_{md3}, \Psi_{mq3}, \Psi_{md5}, \Psi_{mq5}]$ are the permanent magnet flux, r_s is the resistance of the stator, ω is the electrical angular velocity.

B. High Frequency Mathematic Model

The d-q voltage expression in (1) can be divided into three parts. Due to the frequency of injected signal for the sensorless control is from 0.5 kHz to 2 kHz, the first part of (1) can be neglected comparing to the second part. Meanwhile, considering the zero or low speed operation, we can ignore the third part [6]. Therefore, the machine model with high frequency can be simplified as follows:

$$\begin{pmatrix} u_0 \\ u_{d1} \\ u_{q1} \\ u_{d5} \\ u_{q5} \\ u_{d3} \\ u_{q3} \end{pmatrix} = r_s \underbrace{\begin{pmatrix} i_0 \\ i_{d1} \\ i_{q1} \\ i_{d5} \\ i_{q5} \\ i_{d3} \\ i_{q3} \end{pmatrix}}_{\text{First}} + \underbrace{\begin{bmatrix} L_0 & 0 & 0 & 0 & 0 & 0 & 0 \\ 0 & L_{d1} & 0 & 0 & 0 & 0 & 0 \\ 0 & 0 & L_{q1} & 0 & 0 & 0 & 0 \\ 0 & 0 & 0 & L_{d5} & 0 & 0 & 0 \\ 0 & 0 & 0 & 0 & L_{q5} & 0 & 0 \\ 0 & 0 & 0 & 0 & 0 & L_{d3} & 0 \\ 0 & 0 & 0 & 0 & 0 & 0 & L_{q3} \end{bmatrix} \frac{d}{dt} \begin{pmatrix} i_0 \\ i_{d1} \\ i_{q1} \\ i_{d5} \\ i_{q5} \\ i_{d3} \\ i_{q3} \end{pmatrix}}_{\text{Second}} - \omega \underbrace{\begin{pmatrix} 0 \\ L_{q1} i_{q1} + \psi_{mq1} \\ -L_{d1} i_{d1} - \psi_{md1} \\ 5L_{q5} i_{q5} + 5\psi_{mq5} \\ -5L_{d5} i_{d5} - 5\psi_{md5} \\ 3L_{q3} i_{q3} + 3\psi_{mq3} \\ -3L_{d3} i_{d3} - 3\psi_{md3} \end{pmatrix}}_{\text{Third}} \quad (1)$$

$$\begin{pmatrix} u_0 \\ u_{d1} \\ u_{q1} \\ u_{d5} \\ u_{q5} \\ u_{d3} \\ u_{q3} \end{pmatrix} = \begin{bmatrix} L_0 & 0 & 0 & 0 & 0 & 0 & 0 \\ 0 & L_{d1} & 0 & 0 & 0 & 0 & 0 \\ 0 & 0 & L_{q1} & 0 & 0 & 0 & 0 \\ 0 & 0 & 0 & L_{d5} & 0 & 0 & 0 \\ 0 & 0 & 0 & 0 & L_{q5} & 0 & 0 \\ 0 & 0 & 0 & 0 & 0 & L_{d3} & 0 \\ 0 & 0 & 0 & 0 & 0 & 0 & L_{q3} \end{bmatrix} \frac{d}{dt} \begin{pmatrix} i_0 \\ i_{d1} \\ i_{q1} \\ i_{d5} \\ i_{q5} \\ i_{d3} \\ i_{q3} \end{pmatrix} \quad (2)$$

III. SEVEN-PHASE MOTOR TORQUE DISTRIBUTION

Considering the non-sinusoidal electromotive force of multiphase machines, the 3rd harmonic current injection can increase the torque density. And there exists mainly two ways for the injection of 3rd harmonic current. Taking into account the constraint of the inverter, the amplitude of the injected current is imposed. When the thermal constraint of the windings is considered, the rms value of the injected current is often imposed.

A. The minimum rms current value method

The injected current with both the fundamental and 3rd harmonic components can be expressed as:

$$i(\theta) = I_a\left(\sin(p\theta) + a\sin(3p\theta)\right) \quad (3)$$

where p is the number of pole pairs, I_a is the amplitude of fundamental current, a is the ratio of the amplitude of 3rd harmonic current to fundamental one, θ is the mechanical angular position.

The rms current value can be expressed as:

$$I_{rms} = \sqrt{I_a^2 + a^2 I_a^2} \quad (4)$$

The electromagnetic torque in [7] is expressed as follows:

$$T = 7R_s l_a N_p\left[B_1 K_{dp1} I_a + aB_3 K_{dp3} I_a\right] \quad (5)$$

Where N_p, R_s, l_a are the number of turns per phase, the stator inner bore radius and the stator active axial length respectively. K_{dp1} and K_{dp3} are the winding factors of fundamental and 3rd harmonic. B_1 and B_3 are the fundamental and 3rd harmonic flux density of the permanent magnets.

It can be seen that the electromagnetic torque of non-sinusoidal machine has two components, which are produced by fundamental current and 3rd harmonic current respectively.

In(6), T_1, T_3 are used to denote the torque contributed by fundamental current and another one contributed by 3rd harmonic current.

$$T = T_1 + T_3 \quad (6)$$

In order to calculate the minimum rms value of current for a given torque, the Lagrange equation is established:

$$\begin{aligned} L(I_a, a) &= \sqrt{I_a^2 + a^2 I_a^2} + \\ &\lambda\left(7R_s l_a N_p\left[B_1 K_{dp1} I_a + aB_3 K_{dp3} I_a\right] - T^*\right) \end{aligned} \quad (7)$$

Where T^* is the given torque value.

Taking the derivative of (7) with respect to I_a, a and λ respectively:

$$\begin{aligned} \frac{dL(I_a, a)}{dI_a} &= 0 \\ \frac{dL(I_a, a)}{da} &= 0 \\ \frac{dL(I_a, a)}{d\lambda} &= 0 \end{aligned} \quad (8)$$

The parameters of a and I_a are then obtained as:

$$\begin{aligned} a &= \frac{B_3 K_{dp3}}{B_1 K_{dp1}} = \frac{E_3}{E_1} \\ I_a &= \frac{B_1 K_{dp1} T^*}{7N_p R_s l_a\left(B_1^2 K_{dp1}^2 + B_3^2 K_{dp3}^2\right)} \end{aligned} \quad (9)$$

Where E_1, E_3 are amplitude of fundamental and 3rd harmonic electromotive force (EMF).

According to(9), with different value of T^*, the ratio of 3rd harmonic to fundamental is constant and can be expressed as:

$$\frac{T_1}{T_3} = \frac{E_1}{E_3 a} = \frac{E_1^2}{E_3^2} \quad (10)$$

B. The minimum amplitude current value method

Taking the derivative of (3) and equal to zero:

$$\frac{di(\theta)}{dt} = I_a p\left[\cos(p\theta) + 3a\cos(3p\theta)\right] = 0 \quad (11)$$

Solving(11), the follows can be obtained,

$$\cos(p\theta) = 0, 0 < a \le \frac{1}{9} \quad (12)$$

$$\cos(p\theta) = \left(\frac{9a-1}{12a}\right)^{\frac{1}{2}}, a > \frac{1}{9} \quad (13)$$

Substituting(12), (13) into(3), the maximum value of current is obtained in different field of a:

$$\hat{I}_m = (1-a) I_a, 0 < a \le \frac{1}{9} \quad (14)$$

$$\hat{I}_m = I_a 8a\left(\frac{1+3a}{12a}\right)^{\frac{3}{2}}, a > \frac{1}{9} \quad (15)$$

We can see that with the variation of a, the formula for amplitude of (3) is also changed. So there exists two values of a for the minimum amplitude of the current.

For the first one, considering(5)(14), the minimum amplitude is obtained:

$$\begin{aligned} \hat{I}_{m-\min} &= \frac{8}{9} I_a = \frac{8}{9} * \frac{T^*}{7R_s l_a N_p\left(B_1 K_{dp1} + aB_3 K_{dp3}\right)} \\ &= \frac{T^*}{7R_s l_a N_p\left(\frac{9}{8} B_1 K_{dp1} + \frac{1}{8} B_3 K_{dp3}\right)} \\ &= \frac{T^* / B_1 K_{dp1}}{7R_s l_a N_p\left(\frac{9}{8} + \frac{1}{8}\frac{E_3}{E_1}\right)}, a = \frac{1}{9} \end{aligned} \quad (16)$$

The ratio of 3rd harmonic to fundamental is constant and can be expressed as:

$$\frac{T_1}{T_3}=\frac{E_1}{E_3 a}=\frac{9E_1}{E_3} \tag{17}$$

For the second one, considering the equation(5)(15), the Lagrange equation is established:

$$\begin{aligned} L(I_a,a)&=I_a 8a\left(\frac{1+3a}{12a}\right)^{\frac{3}{2}}+\\ &\lambda\left(7R_s l_a N_p\left[B_1K_{dp1}I_a+aB_3K_{dp3}I_a\right]\text{-}T^*\right)\end{aligned} \tag{18}$$

Taking the derivative of (18) with respect to I_a, a, λ and make them to be zero respectively:

$$a=\frac{1}{6-3\dfrac{B_3K_{dp3}}{B_1K_{dp1}}}=\frac{1}{6-3\dfrac{E_3}{E_1}} \tag{19}$$

$$I_a=\frac{3T^*\left(2B_1K_{dp1}-B_3K_{dp3}\right)}{14R_s l_a N_p B_1K_{dp1}\left(3B_1K_{dp1}-B_3K_{dp3}\right)} \tag{20}$$

Substituting (5) into (15) the minimum amplitude is obtained as:

$$\begin{aligned}\hat{I}_m&=I_a 8a\left(\frac{1+3a}{12a}\right)^{\frac{3}{2}}\\ &=\frac{T^*}{7R_s l_a N_p\left(B_1K_{dp1}+aB_3K_{dp3}\right)}*8a\left(\frac{1+3a}{12a}\right)^{\frac{3}{2}}\\ &=\frac{T^*/B_1K_{dp1}}{7R_s l_a N_p\left(1+a\dfrac{E_3}{E_1}\right)}*8a\left(\frac{1+3a}{12a}\right)^{\frac{3}{2}}\end{aligned} \tag{21}$$

According to(19), the ratio of 3rd harmonic to fundamental is constant and can be expressed as:

$$\frac{T_1}{T_3}=\frac{E_1}{E_3 a}=6\frac{E_1}{E_3}-3 \tag{22}$$

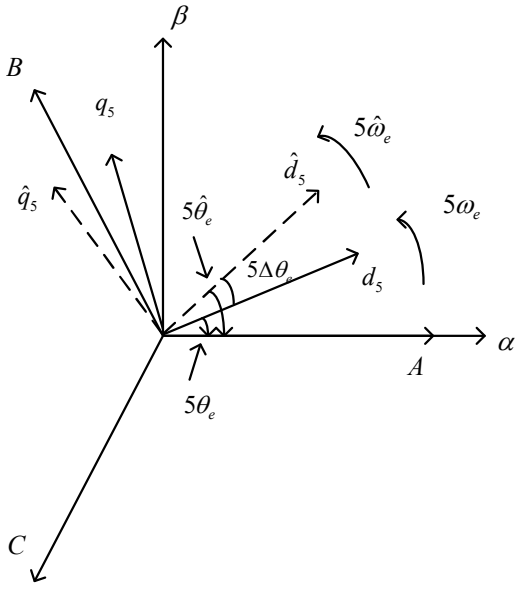

Figure 1 Coordination relationship

IV. HFSI Sensorless Control

A. Coordinate relationship

The coordinate relationship used in sensorless control is expressed in Fig. 1.

Where $\hat{d}$-$\hat{q}$ is estimated d-q coordinate, $\hat{\omega}_e, \hat{\theta}_e$ are estimated electrical angular velocity, estimated electrical rotor position, respectively, $\Delta\theta$ is the error of the real angle to estimated angle.

Due to the estimation of rotor position, there exists a new $\hat{d}$-$\hat{q}$ coordination. The high frequency pulsating voltage signal is injected on the estimated $\hat{d}$ axis. When the $\Delta\theta$ is equal to zero, the $\hat{d}$-$\hat{q}$ coordination is coincident with the d-q coordinate.

B. HFSI theory

The high frequency pulsating voltage signal is injected on the estimated $\hat{d}$ axis.

$$\begin{pmatrix}\hat{u}_{d5h}\\ \hat{u}_{q5h}\end{pmatrix}=\begin{pmatrix}u_{inj}\cos\omega_h t\\ 0\end{pmatrix} \tag{23}$$

Transforming the voltage from estimated rotating coordination to real rotating coordination.

$$\dot{u}_{5h}=u_{inj}\cos\omega_h t\cdot e^{j(5\hat{\theta}_e-5\theta_e)} \tag{24}$$

Substituting (24) into fundamental subspace of(2), the high frequency current is obtained as:

$$\begin{aligned}\hat{i}_{d5h}&=\frac{u_{inj}\sin\omega_h t}{2\omega_h L_{d5}L_{q5}}\left(\left(L_{q5}+L_{d5}\right)+\left(L_{q5}-L_{d5}\right)\cos 10\Delta\theta\right)\\ \hat{i}_{q5h}&=\frac{u_{inj}\sin\omega_h t}{2\omega_h L_d L_q}\left(L_{q5}-L_{d5}\right)\sin 10\Delta\theta\end{aligned} \tag{25}$$

It can be seen that when $\Delta\theta=0$, the $\hat{\imath}_q=0$, $\hat{\imath}_d\neq 0$. Therefore, the $\hat{\imath}_q$ can be taken as an input signal to phase-locked loop (PLL) in order to estimate the position. A band-pass filter (BPF) is used to obtain high frequency signal and demodulating the sinusoidal signal to a DC signal.

$$\begin{aligned}\varepsilon&=LPF\left(\hat{i}_{q5h}\sin\omega_h t\right)\\ &=LPF\left(\frac{u_{inj}\left(L_{q5}-L_{d5}\right)}{2\omega_h L_{d5}L_{q5}}\sin 10\Delta\theta\frac{1-\cos 2\omega_h t}{2}\right)\\ &=\frac{u_{inj}\left(L_q-L_d\right)}{4\omega_h L_d L_q}\sin 10\Delta\theta\end{aligned} \tag{26}$$

The error signal is taken as the input of PLL, the estimated rotor position and estimated angular velocity are thus obtained.

The principle of HFSI is shown in Fig. 2.

V. Simulation

The simulation verification is divided into two parts, one is the decoupling control of non-sinusoidal motor in multi-subspace. Another one is sensorless control using HFSI.

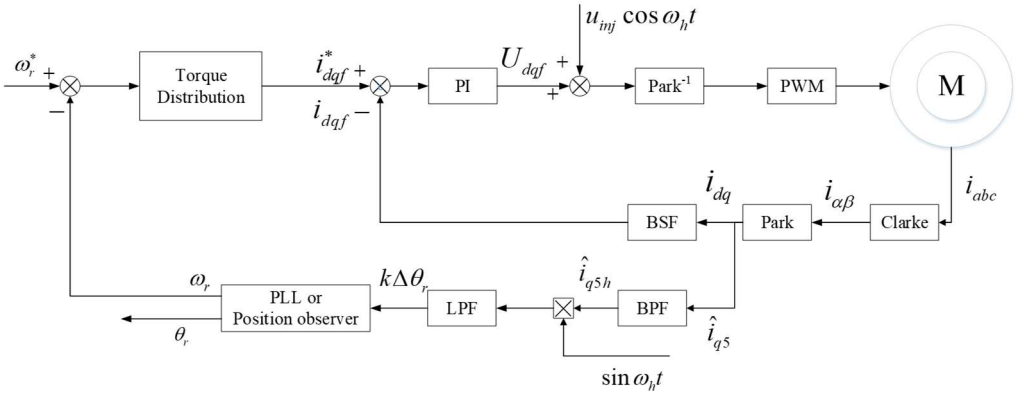

Figure 2 Pulse high frequency signal injection method

A. Decoupling Control

The output torque of the non-sinusoidal multiphase machine can be obtained through the injection of current in fundamental subspace or the third harmonic subspace, which can be controlled independently[8].In simulation, the machine parameters used for simulation is shown in TABLE I.

TABLE I. PARAMETERS OF SNPMSM

Parameter	symbol	Value
Rated speed	$n_N(rpm)$	600
Pole-pairs	p	6
Rotational inertia	J (kg.m^2)	0.02
Resistance per phase	R_s (Ω)	0.67
Fundamental permanent magnetic flux	Ψ_1 (wb)	0.1146
Third harmonic permanent magnetic flux	Ψ_3 (wb)	0.0446
Fundamental subspace d-axis inductance	L_{d1}(mH)	4.4383
Fundamental subspace q-axis inductance	L_{q1}(mH)	4.6900

According to the finite element analysis (FEA), the ratio of 3rd harmonic EMF to fundamental one of the studied seven-phase non-sinusoidal machine is:

$$\frac{E_3}{E_1}=\frac{0.4740}{0.4038}=1.1738 \tag{27}$$

Substituting (27) into (16) and substituting (27), (19) into (21), the minimum amplitude in different filed is obtained:

$$\begin{aligned}\hat{I}_{m-\min 1}&=0.7863*\frac{T^*/B_1K_{dp1}}{7R_sl_aN_p},a=\frac{1}{9}\\ \hat{I}_{m-\min 2}&=0.6757*\frac{T^*/B_1K_{dp1}}{7R_sl_aN_p},a=0.4035\end{aligned} \tag{28}$$

It can be seen that the second amplitude is smaller than first one. In this simulation, the second torque distribution with minimum amplitude is used.

The simulation time is set as 0.05s, the reference torque as 10N•m. The torque decoupling control result is shown in Fig. 3 and Fig. 4 with two torque distribution methods.

From the simulation results, it can be seen that the sum of the subspace torque value is the same as electromagnetic torque value. So the electromagnetic torque can be controlled by different subspace in a decoupled way.

The waveform of current in phase A is shown in Fig. 5 and Fig. 6.

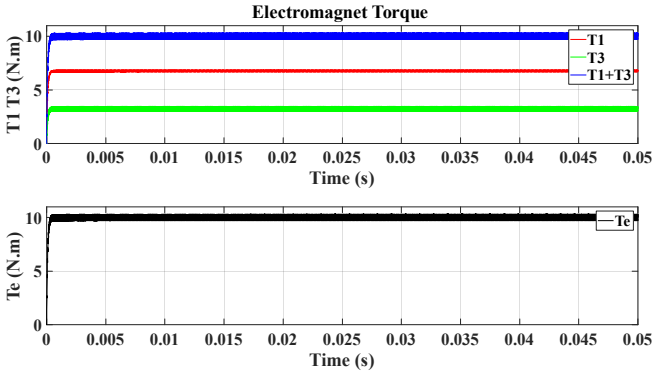

Figure 3 Electromagnetic torque and sum of subspace torque with minimum amplitude

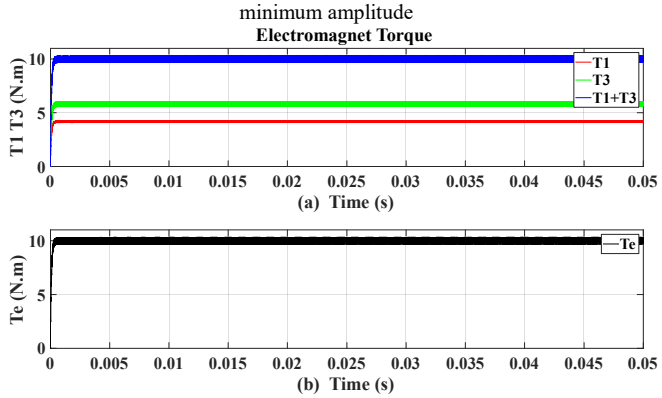

Figure 4 Electromagnetic torque and sum of subspace torque with minimum rms

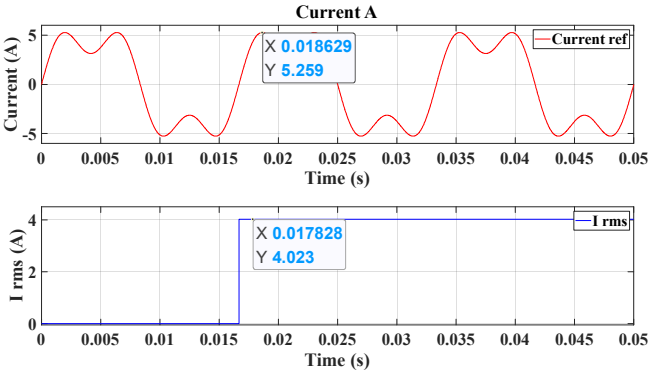

Figure 5 The Current of A and its rms with minimum amplitude

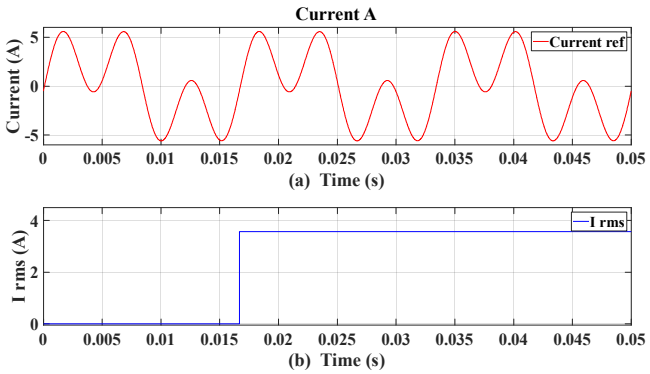

Figure 6 The Current of A and its rms with minimum rms

Comparing the two figures, it can be seen that the current amplitude with minimum amplitude method is smaller than the minimum rms method, which can satisfy the constraint of inverter more easily. But the rms with minimum amplitude method is larger which means the thermal constraint is challenged. The method with minimum rms is opposite of minimum amplitude method, which satisfies the thermal constraint more easily and is challenged in inverter constraint. In practical application, the proper torque distribution method should be selected by specific constraints and requirements.

B. Sensorless Control

The HFSI method in fundamental subspace and 5th harmonic subspace are simulated respectively. The simulation time is 20s and is started with no-load. 2N•m load torque is added to simulation gradually.

The result of speed and position estimation in fundamental subspace is shown in Fig. 7, and Fig. 8. And the 5th harmonic subspace's is shown in Fig. 9 and Fig. 10.

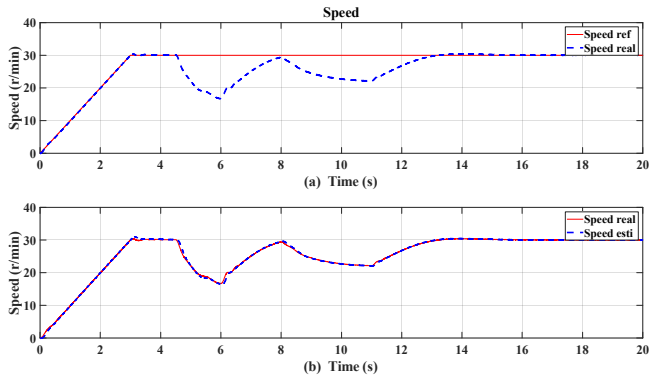

Figure 7 Speed estimation in fundamental subspace

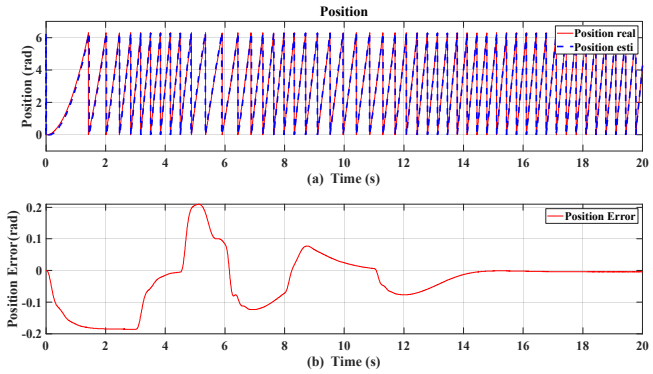

Figure 8 Position estimation in fundamental subspace

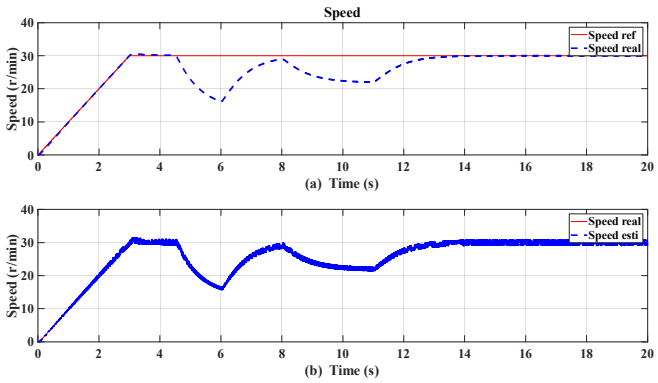

Figure 9 Speed estimation in 5th harmonic subspace

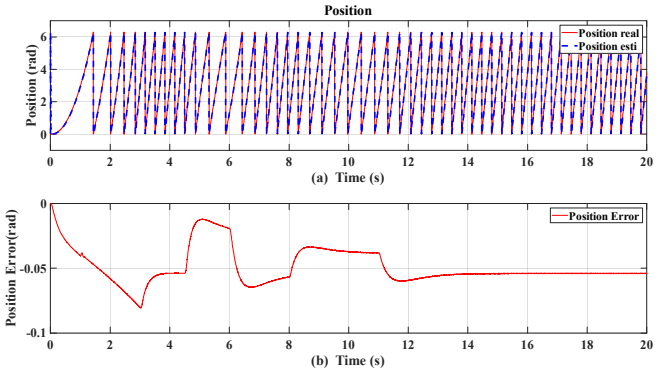

Figure 10 Position estimation in 5th harmonic subspace

As we can see, both with two methods, the machine can start with zero to low speed slowly. And in low speed operation, the torque can be add gradually with the machine keeping stabilization. The maximum position estimation error is 0.2rad with fundamental method. And the 5th one is 0.1 rad.

The torque ripple with two methods is given in Fig. 11 and Fig. 12.

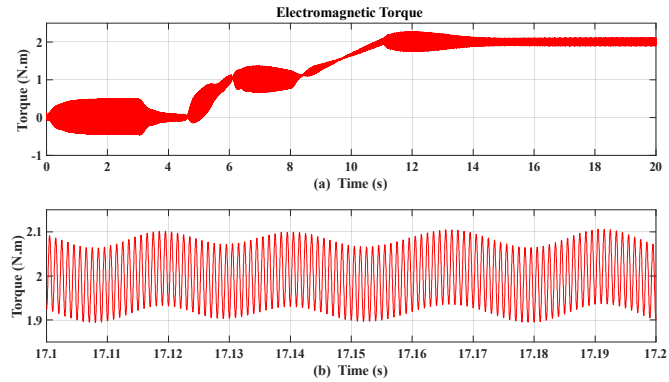

Figure 11 Torque ripple in fundamental subspace

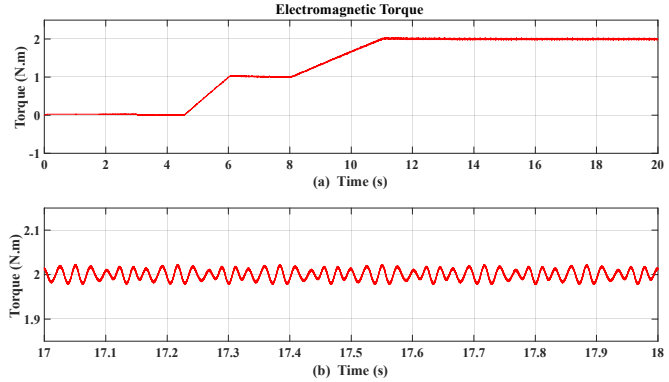

Figure 12 Torque ripple in 5th harmonic subspace

The torque ripple with the sensorless control in fundamental subspace is 10%, and with the sensorless control in 5th harmonic subspace is 2.25%. The torque ripple is reduced by proposed method.

VI. Conclusion

This paper deduces two torque distribution methods in operation with minimum rms and amplitude value of current. The waveform with two methods is given. The result shown the two methods have their strengths. In practical application, the proper torque distribution method should be selected by specific constraints and requirements. And also, a high frequency signal injection is proposed in non-sinusoidal in fundamental subspace, which can reduced the torque ripple caused by injected signal.

References

[1] E. Levi, F. Barrero and M. J. Duran, "Multiphase machines and drives - Revisited," *IEEE Transactions on Industrial Electronics,* vol. 63, pp. 429-432, 2016-01-01 2016.

[2] E. Levi, N. Bodo, O. Dordevic, and M. Jones, "Recent advances in power electronic converter control for multiphase drive systems," in *2013 IEEE Workshop on Electrical Machines Design, Control and Diagnosis (WEMDCD)*, 2013, pp. 158-167.

[3] D. A. T. Guzman, N. K. Nguyen, M. Trablesi, and E. Semail, "Low Speed Sensorless Control of Non-Salient Poles Multiphase PMSM," in *2019 IEEE International Conference on Industrial Technology (ICIT)*, 2019, pp. 1563-1568.

[4] G. Wang, D. Xiao, G. Zhang, C. Li, X. Zhang, and D. Xu, "Sensorless Control Scheme of IPMSMs Using HF Orthogonal Square-Wave Voltage Injection Into a Stationary Reference Frame," *IEEE Transactions on Power Electronics,* vol. 34, pp. 2573-2584, 2019-01-01 2019.

[5] J. Gong, H. Zahr, E. Semail, M. Trabelsi, B. Aslan, and F. Scuiller, "Design Considerations of Five-Phase Machine With Double p/3p Polarity," *IEEE Transactions on Energy Conversion,* vol. 34, pp. 12-24, 2019-01-01 2019.

[6] G. Liu, C. Geng and Q. Chen, "Sensorless Control for Five-Phase IPMSM Drives by Injecting HF Square-Wave Voltage Signal into Third Harmonic Space," *IEEE Access,* vol. 8, pp. 69712-69721, 2020-01-01 2020.

[7] K. Wang, D. S. Lin, P. Zhou, Z. Q. Zhu, and S. Zhang, "Analytical determination of 3rd order harmonic current into five phase PM machine for maximum torque," in *2015 IEEE International Electric Machines & Drives Conference (IEMDC)*, 2015, pp. 630-636.

[8] E. Semail, X. Kestelyn and A. Bouscayrol, "Right harmonic spectrum for the back-electromotive force of an n-phase synchronous motor," in *Conference Record of the 2004 IEEE Industry Applications Conference, 2004. 39th IAS Annual Meeting.*, 2004, pp. 1-78.